Pure Magnetooptic Diffraction and Kerr Microscopy of Periodic Domain Structures

J. L. Costa-Krämer, A. Bengoechea, R. Alvarez-Sánchez, and F. Briones

Instituto de Microelectrónica de Madrid, IMM-CNM-CSIC, 28760 Tres Cantos, Madrid, Spain

The fabrication of a periodic domain structure in a ferromagnetic thin film is reported. This periodic domain structure is formed in a thin continuous magnetic film by coupling it to a periodic array of magnetic elements grown on top. When the array and the continuous film are exchange decoupled, magnetostatic interactions produce in the continuous layer a domain structure replica of the topographic pattern at selected field values. The present work reports a direct confirmation of this periodic domain structure in the flat continuous film by Kerr microscopy, which is responsible for the pure magnetooptic diffraction. The effect on the magnetization processes of one- and two-dimensional structures with different periodicities and dimensions is studied in detail and compared with micromagnetic simulations, for Co and Fe films.

***Index Terms*—Diffraction, magnetic domains, magnetooptic Kerr effect.**

I. Introduction

CONVENTIONAL magnetooptic (MO) techniques, and more recently, diffraction magnetooptic Kerr effect (DMOKE) [1]–[17] on regular arrays of magnetic elements, are very powerful methods that possess the high sensitivity required to monitor magnetization changes in thin films and very small elements of different shapes. Most of these works focus on structures consisting on arrays of isolated magnetic elements over a nonmagnetic substrate. Much less work has been devoted to arrays of magnetic elements over a continuous magnetic layer. A recent work [17] has reported the appearance of diffraction spots at selected field values when illuminating a flat Co ferromagnetic surface that is magnetically coupled to an array of magnetic elements. This study is carried out by growing on top of a transparent substrate a continuous magnetic film—thick enough to be opaque to the light used in MO characterization—and an array of magnetic elements on top of this continuous magnetic layer. This type of structure allows magnetooptic measurements both when illuminating from the patterned side or from the flat side (Fig. 1). At magnetic saturation, the patterned side reflects and diffracts while the flat side just reflects. The diffraction spots appearing when illuminating the flat side at selected field values are tentatively attributed to a periodic domain structure in the flat continuous magnetic film. This assumption is supported by the different magnetic behaviors observed when the magnetic two-dimensional (2-D) array is exchange coupled or decoupled to the continuous magnetic film, and by micromagnetic simulations. Indeed, the angular position of this diffraction spot corresponds to the periodicity of the array.

The present work confirms by direct Kerr domain observations that these diffraction spots are originated from the periodic domain structures that appear at selected field values. At these field values, when the array and the film are exchange-decoupled, the magnetization in the continuous film area under the element orients antiparallel to the array elements magnetization. Accordingly, the domain structures replicate the topographic pattern created on top of the continuous film. These induced domain structures are due to the reduction in magnetostatic energy between the magnetic elements of the pattern and the continuous film. The samples studied in [17] were arrays of Co stripes on top of a continuous Co layer, i.e., a one-dimensional (1-D) pattern. This work presents an extended study for 1-D and 2-D arrays using both Co and Fe to fabricate the structures.

II. Fabrication

The type of structures under study consists of an array of magnetic elements on top of a continuous magnetic layer grown on a transparent nonmagnetic substrate, allowing the MO characterization illuminating from either side of the structure. From now on, the two sides of the sample will be termed the *patterned* and the *flat* sides. Two types of structure will be discussed in detail: arrays of Co microstripes on top of a continuous Co layer (1-D heterostructures) and arrays of Co (Fe) microsquares on top of continuous Co (Fe) (2-D heterostructures). Typical array element sizes and array periodicities are in the micrometer range. This size allows magnetic domain visualization with a conventional Kerr microscopy setup, and the array periodicity generates diffracted beams at conveniently spaced angles.

A. 1-D Heterostructures Fabrication

Our 1-D heterostructures are microfabricated by optical lithography on polycrystalline Co sputtered on glass. First, a 80-nm-thick Co continuous layer is grown by triode dc sputtering. This thickness guarantees optical opacity for a 633-nm-wavelength 1.5-mW laser light. The transmittance of this film was measured to be less than 10^{-5}.

The deposited Co layers exhibit uniaxial anisotropy field in the direction of the plasma confining field during sputtering, with an anisotropy field of 30 Oe. On top of the continuous Co layer, a stripe array is performed by optical lithography followed by a second 160-nm-thick Co sputtering deposition and a lift-off. The mask used consists of stripe patterns with widths in the range 2–100 μm and interstripe spacings from 4 to 8 μm. Specifically, the patterns used are $100\_8, 50\_8, 25\_8, 12\_3, 6\_3, 4\_4, 2.5\_4$, where the first number

Digital Object Identifier 10.1109/TMAG.2005.856168

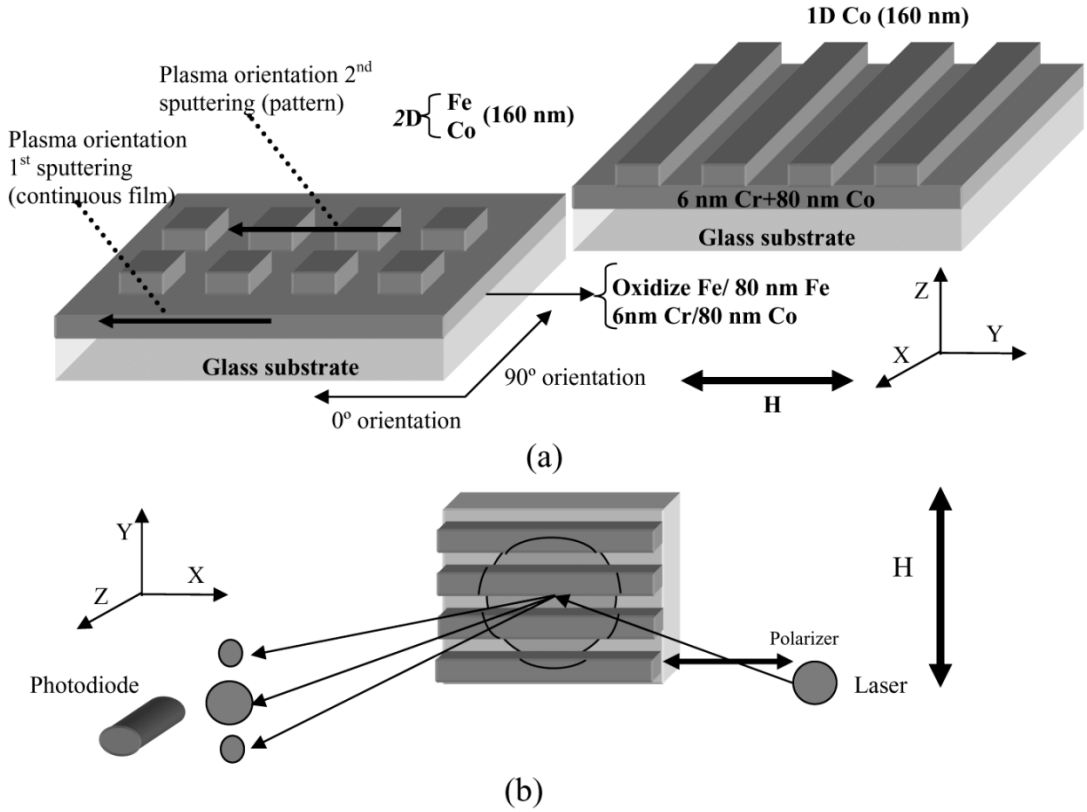

Fig. 1. (a) Sketch of the studied heterostructures. The microelement arrays are fabricated by e-beam lithography (2-D case) or optical lithography (1-D case) on a sputtered continuous 80-nm-thick layer. In both cases, the lithography is followed by a second sputtering deposition (160 nm) and a lift-off. The glass substrate allows MO caracterization at both sides of the heterostructure. (b) Sketch of the experimental transversal Kerr setup for a 1-D heterostructure in 0° orientation.

denotes the stripe width and the second the stripe to stripe separation, both in micrometers.

The easy magnetization axis of the sputtered Co can be parallel or perpendicular to the stripe long axis. Our heterostructures labeling is defined as follows: first the array width, then the array interspacing and finally the direction of the Co anisotropy axes with respect to the stripe long axis for both the continuous layer and the stripe pattern, using Pe for perpendicular and Pa for parallel. This way, the structure called "50_8 *PePe*" is a sample in which: 1) the stripes are 50 μm width separated 8 μm and 2) the anisotropy of the continuous Co is perpendicular to the stripe long axis in both the continuous layer and the stripe pattern. However, "50_8 *PaPe*" represents a structure with the same dimensions but with the anisotropy of the continuous Co layer parallel to the stripe long axis.

B. 2-D Heterostructures Fabrication

The second type of samples are 2-D arrays of Fe (Co) squares on top of a continuous Fe (Co) layer. The Fe continuous layer is also grown by dc triode sputtering and has an anisotropy field of 10 Oe. The arrays consist of squares of edge size in the range 80–15 μm, and intersquares width from 20 to 3 μm. Assuming the same 1-D heterostructures labeling, the following 2-D structures are fabricated: 80_20, 60_10, 30_5 and 15_3. The microstructured arrays are fabricated by e-beam lithography over a 1.2 μm PMMA thick layer, in a 400×400 μm^2 working area.

In the case of the structures created by optical lithography (1-D heterostructures), a thin oxide layer is created during developing. This oxide layer exchange-decouples the stripes array from the continuous film. For the structures created by e-beam lithography (2-D heterostructures), the square array is exchange-decoupled from the continuous film by an intermediate 6-nm-thick sputtered Cr layer (for Co/Cr(6 nm)/2DCo structures) or by an Fe oxide layer grown by an oxygen plasma at 50 W during 5 min (for Fe/oxid.Fe/2DFe structures).

III. Measurements and Discussion

Transverse magnetooptic Kerr effect (TMOKE) measurements are performed by illuminating with a 632.8 nm He–Ne laser both sides of our heterostructures. The incidence angle is 60°, and the spot diameter is focused within the patterned area. This spot size is chosen to be around 1 mm^2, in the case of 1-D Co heterostructures, and 250×250 μm^2 for 2-D heterostructures in order to assure that the measured MOKE signal is an average of the whole sample. The magnetic field is applied perpendicular to the stripes long axis in 1-D structures and parallel to both square edge directions in 2-D structures. Fig. 2 reviews conventional MOKE measurements (at reflected beam) for "Co/1D Co" heterostructures. The left side shows the hysteresis loops—when illuminating at both the flat and the patterned sides—obtained for the heterostructures whose easy axis is perpendicular to the stripe long axis (PePe structures). The right side shows the result for the structures with the stripes Co easy axis parallel to the stripe long axis (PaPe structures). The applied magnetic field is enough to achieve magnetic saturation except perhaps for the narrowest stripes (4_4 mm and 2.5_4 mm structures).

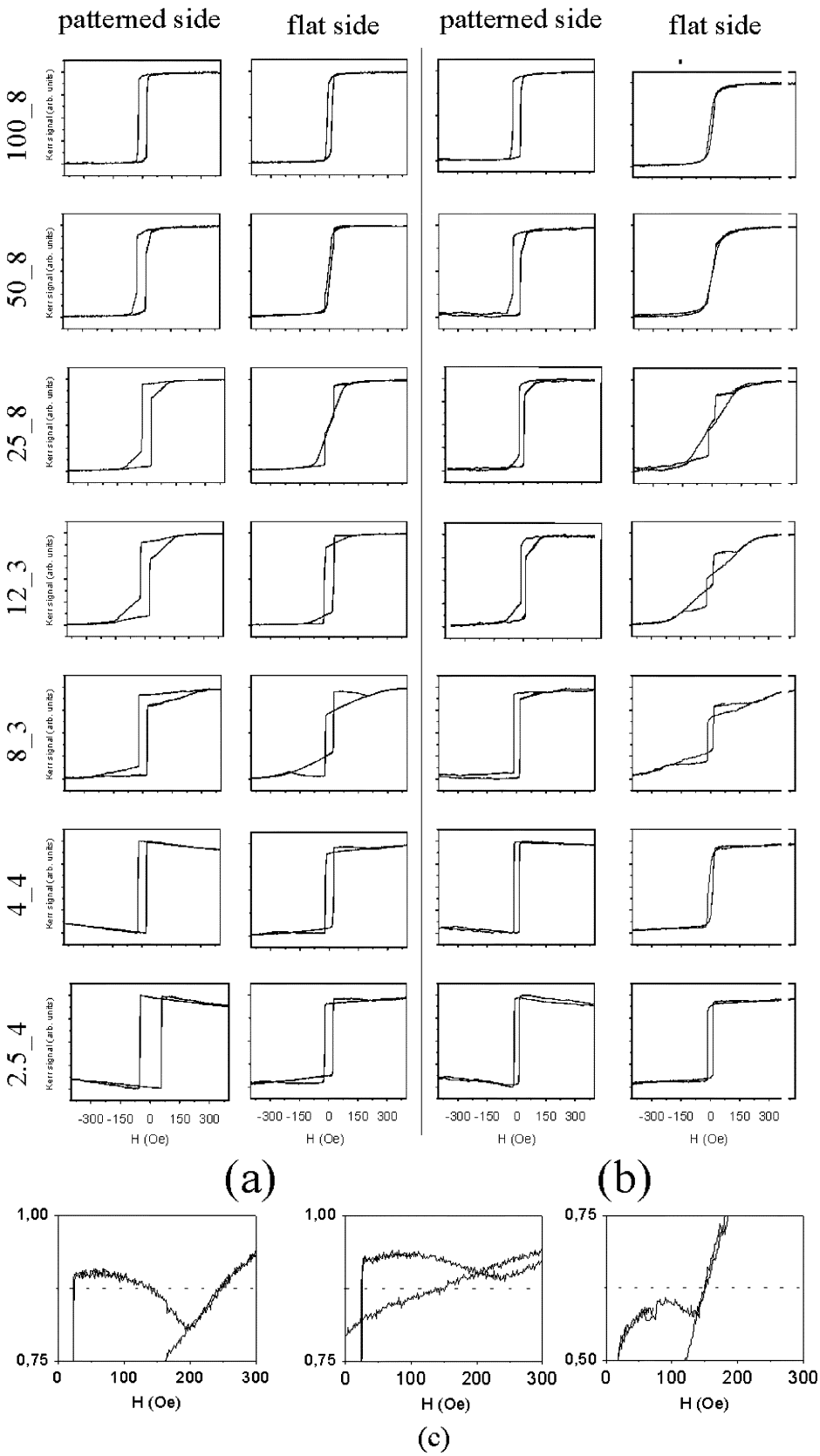

Fig. 2. Conventional MOKE measurements (relative magnetization M/M_S versus external field H) for the structures Co/1D Co, illuminating at both sides of the sample. (a) ("PePe" structures.) The Co anisotropy for both the stripes and continuous layer are perpendicular to the stripes long axis. (b) ("PaPe" structures.) The easy axis for the Co stripes is parallel to the stripes, but the continuous layer anisotropy remains perpendicular to the stripes. (c) Details of "8_3 PePe," "4_4 PePe," and "12_3 PaPe" hysteresis loops that exhibit a negative differential susceptibility when illuminating at the flat side.

From Fig. 2, it is clear that the hysteresis loops illuminating each side of the structure are different. This is consistent with the fact that the microelement arrays are exchange-decoupled from the continuous layer. The continuous layer is opaque at

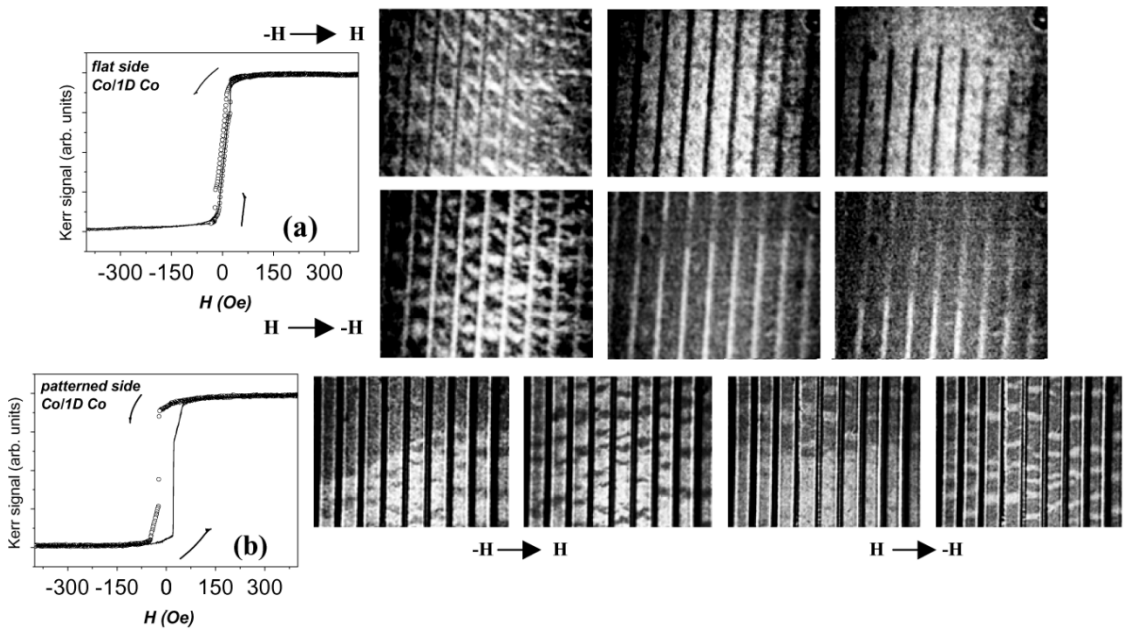

Fig. 3. Magnetic domain images related to conventional hysteresis loops for the structure "50_8 *PePe* (Co/1D Co)," illuminating either at flat (a) and patterned (b) sides. Images show some domain distributions when the applied field drives the magnetization from positive saturation to negative saturation and back. Observing through the glass, we can see that a periodic domain structure is generated in the flat ferromagnetic film at certain field values (a).

this wavelength, and consequently when illuminating the patterned side we obtain information about the stripes magnetization plus the interstripe contribution. But when illuminating the flat side only, the continuous film magnetization is measured. The saturation field increases as the stripe width decreases as expected from magnetostatic considerations. On the other hand, the stripes' easy axis orientation with respect to the anisotropy axis of the continuous layer does not seem to play an important role as the corresponding measured PePe and PaPe loops are qualitatively similar. For bigger stripe lateral dimensions and interstripe spacing, the coercive field varies in a narrow range of approximately 17 Oe, but the saturation field is quite sensitive to these changes.

There are also some interesting features that deserve to be examined in detail. Some of these structures, when being illuminated at its flat side, shows hysteresis loops with a negative differential susceptibility [see Fig. 2(c)]. This points to the growth of domains with the magnetization oriented opposite to the applied magnetic field direction. The most plausible explanation of this behavior is the formation of an inversion domain underneath the stripe, due to the magnetostatic energy reduction. This inversion domain, being regularly spaced under the stripes, would be as well responsible for the measured pure magnetooptic diffraction reported in [17]. In order to confirm this assumption, a homemade Kerr domain observation microscope [18] was used. A Xe lamp was used as a light source, and a polarizer and an analyzer were placed at almost extinction condictions in the longitudinal Kerr configuration. The changes of the polarization rotation—now spatially resolved—are recorded by a digital video camera. After recording a whole loop, which takes 100 s, the video has been edited and certain frames have been selected for further image processing. The processing consists of a contrast enhancement by subtracting the domain image at a certain field value and the saturated sample image. Due to the spatial resolution of our system (around 10 μm), only structures over 25 μm stripe width were measured.

In Fig. 3, domain images at selected field values are shown for the "50_8 PePe" heterostructures together with the corresponding hysteresis loops. As shown before the anisotropy orientation for the Co layers in the structure "Co/1D Co" plays a minor role, so we will restrict our discussion from now on to heterostructures with both easy-axis perpendicular to the stripes' long axis ("PePe"). In the Kerr microscope the information contained in the hysteresis loop is spatially resolved, so we can see that magnetization reversal takes place by the nucleation and growth of inversion domains. In Fig. 3(b), the stripes' domain structure in the patterned side clearly show black and white domains whose orientation is parallel and antiparallel to the applied field, respectively. These domains are separated by 180° domain walls, and depending on the applied field direction, one type of domain grows at the expense of the other. When looking at the magnetization reversal process at the flat side of the heterostructure [Fig. 3(a)], similar domain structures are observed in the area underneath the stripes. The behavior of the interstripe area is markedly different, and all the interstripe areas seem to behave coherently. More significant is that at selected field values a domain replica of the periodic topographic structure is observed, i.e., all the magnetization under the stripe is aligned antiparallel to the interstripe area. This is a pure magnetooptic grating. Taking into account that when the sample is saturated the continuous layer only reflects, illuminating one of these periodic domain structures, diffraction spots at regular positions corresponding to the pattern periodicity are expected to appear.

Figs. 4 and 5 show the results for similar measurements in "Co/2D Co" and "Fe/2D Fe" structures. The fabrication processes for these heterostructures guarantee again that exchange coupling is not operative between the pattern and the continuous layer. For the 2-D heterostructures, the field is applied parallel to one square edge. This produces magnetic poles at saturation at the surfaces perpendicularly oriented to the applied field. In Fig. 5 ("Fe/2D Fe" structure) both the 0° and 90° orientations shows similar domain structures during a complete field cycle,

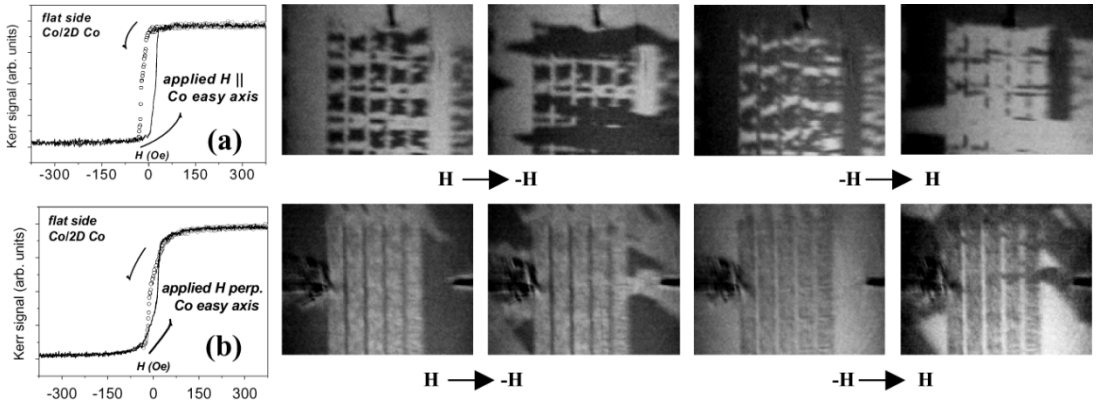

Fig. 4. Hysteresis loops and domain images at selected field values for heterostructures 60_10 (Co/2D Co) illuminated through the glass substrate. (a) Images when the external field is applied parallel to Co easy axis and (b) when the external field is applied perpendicular to Co easy axis. Notice the different patterns when applying the field perpendicular or parallel to the Co anisotropy axis.

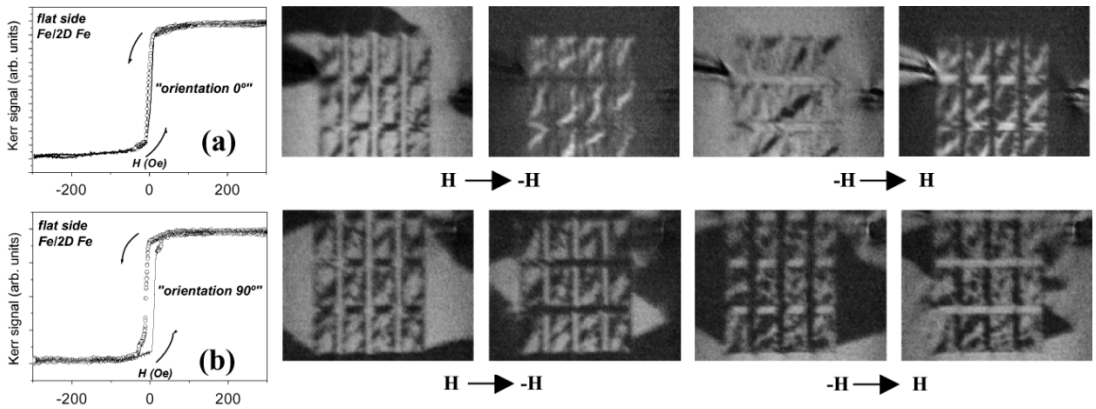

Fig. 5. Hysteresis loops and domain images at selected field values for heterostructures 80_20 (Fe/2D Fe) illuminated through the glass substrate. (a) Images when the external field is applied parallel to one edge (labeled "0° orientation") and (b) when the external field is applied perpendicular to the other edge ("90° orientation").

whereas in the case of "Co/2D Co" the domain structures are not similar (see Fig. 4). This might be due to small differences in the interelement distances along different directions or, most probably, to the effect of the Co uniaxial anisotropy (anisotropy field of 30 Oe) which in this case is parallel to one of the edges (and parallel to the applied external field in Fig. 4(a). The most clear periodic domain structures are observed when applying the field perpendicular to the Co easy axis [Fig. 4(b)].

In all cases, the inversion process is as follows: First, an inversion underneath the topographic pattern followed by a domain nucleation and propagation. This domain propagation is responsible for the big jumps observed in the hysteresis loops.

The images in Figs. 4 and 5 are taken in the nearby of the 0 Oe field, just before and after the big jumps in the hysteresis loops occur.

As demonstrated, the fabrication of heterostructures consisting of a periodic topographic pattern over a continuous film produces at special field values periodic domain structures in the flat film. These periodic domain structures are expected to diffract, and this may be observed even with the eye with the help of a diffusive screen. Once localized these diffraction spots that blink much like a lighthouse when the magnetic field switches the photodiode can be placed at this angular position and the diffracted light dependence on the applied magnetic field can be measured. The dependence of the first order diffracted light on the applied magnetic field is shown in Fig. 6 (see Figs. 2–5 for zero-order loops) for different structures: Fig. 6(a) "Co/1D Co," Fig. 6(b) "Co/2D Co," and Fig. 6(c) "Fe/2D Fe." In the latter case, we also show the first-order diffraction spot intensities dependencies in the 90° orientation [see Fig. 1(a) for details]. Turning back to the domain images ("Co/1D Co" and "Co/2D Co" structures in Figs. 3 and 4), the induced periodic domain structure at the flat ferromagnetic film ought to lead to a diffraction spot that appears twice per field cycle and, due to the symmetry, it should be an even function of the applied magnetic field. This is expected since the reflectivity, in the transversal Kerr configuration, depends only on the magnetization component along the applied field direction. The experimental findings shown in Fig. 6 do not agree with this fact. The reason for this behavior is not clear yet, and it might be due to a variety of reasons that are currently under investigation. Notice, however, that the first loop shown in Fig. 6(b) resembles very much an even function of the field with a small odd function superimposed. This could be due to the presence of diffused light, besides the diffracted light, that also carries a magnetooptic component. Supporting this statement, notice that in none of the cases the diffracted light vanishes at magnetic saturation as seen in the hysteresis loops in the reflected spots. This would indicate that either the sample is not "technically" saturated, having small closure domains,

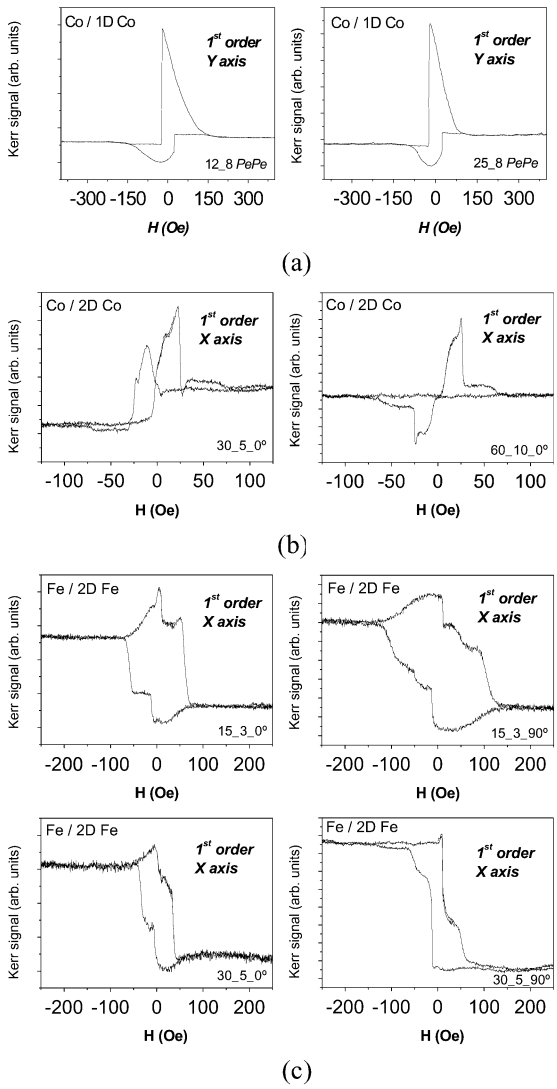

Fig. 6. Magnetooptically diffracted light dependencies for different heterostructures. The first Y order (out of incidence plane) is presented for (a) "Co/1D Co," and first X order (in the incidence plane) for (b) "Co/2D Co" and (c) "Fe/2D Fe" structures. We have measured the "Fe/2D Fe" structures for the two orientations parallel to the edges of the square elements (labeled 0° and 90° orientations). The corresponding zero-order loops are shown in Fig. 2.

or that although our continuous film is opaque, there are small variations in the reflectivity (in principle less than 10^{-5}) between the area under the stripes and the interstripe area that diffract light even at magnetic saturation.

IV. Micromagnetic Simulations

The experimental findings described so far are correlated with micromagnetic simulations performed with the OOMMF 1.1b code [19] with 3-D spins in a 2-D mesh. The 2-D mask used represents the cross section of the stripes array period. Thus, according to the chosen axis notation and to the way OOMMF performs calculations in a 2-D mesh using the FastPipe Demag specification, the direction along the stripe (X-axis direction) is supposed to be infinite. Even with this simple model, the experimental results might be reproduced. As an example, results for a heterostructure consisting of 4-μm-wide stripes and 4-μm-wide interstripe with infinite long stripe axis are presented in Fig. 7(a), where the magnetization at different H values are shown for the cross section of one period of the 1-D array. The stripes in this case are exchange-decoupled by removing one layer of magnetic elements between the stripes and continuous film. Fig. 7(a) shows the magnetization component along the applied field direction (field applied in the horizontal page direction) in a complete field cycle (both H to $-H$ and $-H$ to H sweeps) at 150 Oe field steps. Notice that twice per loop an inversion domain forms at the continuous layer area under the stripes [Fig. 7(a)]. This occurs when the understripe orients antiparallel to the stripe magnetization—that remains parallel to the field—in order to reduce the magnetostatic energy. As the Co anisotropy axis lies along the stripe long direction, the combined effect of crystalline anisotropy and shape anisotropy makes the stripe magnetization remain parallel to the field longer. Notice as well that due to the double thickness of the stripe, its weight in the potential energy is larger. This is supported by experiments in which the continuous layer and the stripe were fabricated with the same thickness. In these experiments, neither this inversion domain in the continuous layer nor the pure magnetooptic diffraction are observed. The hysteresis loops obtained when illuminating from both sides deduced from the micromagnetic simulation data are also shown in Fig. 7(a). Note the experimentally observed negative differential susceptibility when illuminating the flat side is reproduced in the simulations. In Fig. 7(b), we show the result of calculating the diffracted light intensity (first order, X direction) using the micromagnetic simulation domain structure and the expression that provides the diffracted intensity from a given magnetization distribution $m_y(x)$ in a periodic structure of period T

$$I_n \propto \left| \int_{-T/2}^{T/2} (1 + A \cdot m_y(x)) e^{i \cdot \frac{n 2\pi x}{T}} \, \mathrm{d}x \right|^2 .$$

Notice that the response is an even function of the field and that the diffraction spot appears twice per loop.

V. Conclusion

We have analyzed in detail the magnetization processes and the magnetooptical behavior of heterostructures consisting of a periodic array of microsized ferromagnetic elements deposited on top of a continuous ferromagnetic film. The 1-D and 2-D patterns are fabricated with sizes in the micrometer range in order to be able to correlate magnetization processes and magnetooptical behavior with domain observations using Kerr microscopy, and to obtain diffraction spots well resolved angularly. Choosing the appropriate thick and lateral dimensions and using a transparent substrate allows the magnetooptical characterization from both sides of the heterostructures. By comparing loops from either side, it is possible to discern if the magnetization behaves coherently along the heterostructures. The present work confirms by Kerr domain microscopy that a regular array of magnetic domains is responsible for a pure magnetooptical diffraction that can be modulated with an applied magnetic field. We have analyzed 1-D and 2-D arrays exchange-decoupled from the continuous film and demonstrated that this fact produces an inversion domain under the patterned magnetic elements due to the magnetostatic energy reduction. These inversion domains create on the flat side of the sample a domain

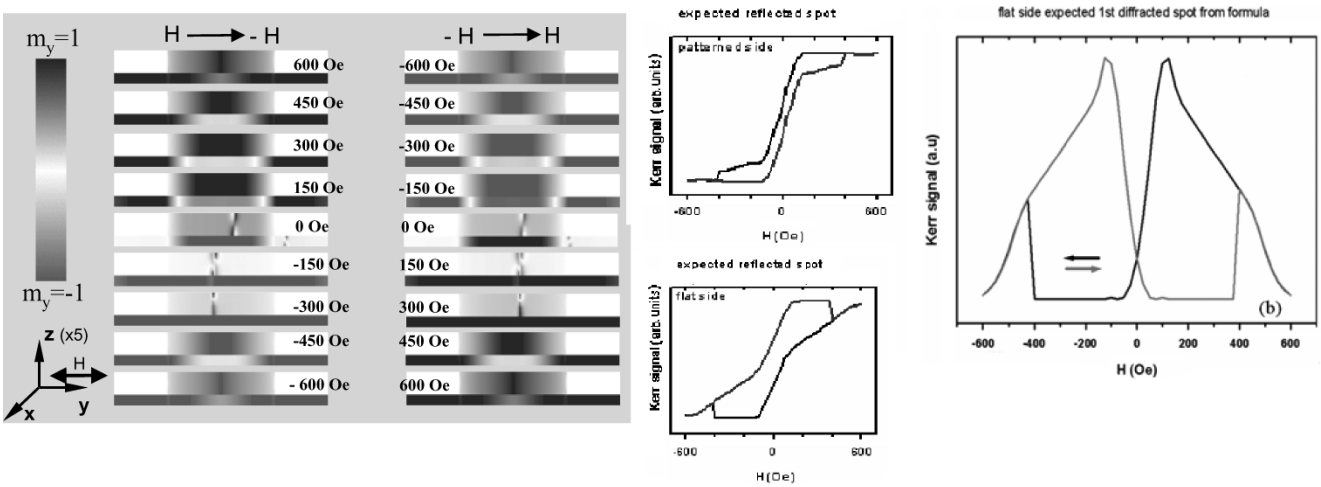

Fig. 7. (a) Micromagnetic simulations for "4_4 Co/1D Co" heterostructure exchange-decoupled from the continuous layer and calculated hysteresis loops for that structure. Illuminating the flat side, the hysteresis loop reproduces the experimentally found negative differential susceptibility. The figure represents the magnetization in the cross section of one period of the array at different external field values for a complete H cycle, i.e., for both H to $-H$ (left) and $-H$ to H (right). In (b), first X order diffracted light intensity expected, when illuminating the flat side.

replica of a lithographically defined pattern. This way, the reported experiments demonstrate the feasibility of transferring a pattern from a mask into a domain structure. Although the diffraction by a periodic domain configuration is demonstrated, the diffracted light dependency on the applied magnetic field does not accurately follow theoretical predictions.

ACKNOWLEDGMENT

This work was supported by the EU project HIDEMAR G5RD-CT-2002-00731. A. Bengoechea acknowledges financial support from the I3P program of Consejo Superior de Investigaciones Científicas (CSIC). R. Alvarez-Sánchez acknowledges a doctoral grant from the Consejería de Educación de la Comunidad de Madrid. The authors would also like to thank S. Melle for the help in constructing the homemade Kerr microscope and P. García-Mochales for the micromagnetic simulations.

REFERENCES

[1] D. Jaque, J. I. Martin, G. Armelles, J. L. Costa-Krämer, F. Briones, and J. L. Vicent, "Nanopatterning effects on magnetic anisotropy of epitaxial F (001) micrometric squares," *J. Appl. Phys.*, vol. 91, pp. 382–388, 2002.

[2] P. Garcia-Mochales, J. L. Costa-Krämer, G. Armelles, F. Briones, D. Jaque, J. I. Martin, and J. L. Vicent, "Simulations and experiments on magneto-optical diffraction by an array of epitaxial Fe (001) microsquares," *Appl. Phys. Lett.*, vol. 81, pp. 3206–3208, Oct. 2002.

[3] O. Geoffroy, D. Givord, Y. Otani, B. Pannetier, A. D. Santos, M. Schlenker, and Y. Souche, "TMOKE hysteresis loops in Bragg diffraction from 2D patterns," *J. Magn. Magn. Mater.*, vol. 121, no. 516R, 1993.

[4] T. Schmitte, O. Schwöbken, S. Goek, K. Westerholt, and H. Zabel, "Magnetooptical Kerr effect of Fe-gratings," *J. Magn. Magn. Mater.*, vol. 240, pp. 24–26, 2002.

[5] T. Schmitte, T. Schemberg, K. Westerholt, and H. Zabel, "Magneto-optical Kerr effect of ferromagnetic Ni-gratings," *J. Appl. Phys.*, vol. 87, p. 5630, 2000.

[6] T. Schmitte, K. Westerholt, and H. Zabel, "Magneto-optical Kerr effect in the diffracted light of Fe gratings," *J. Appl. Phys.*, vol. 92, pp. 4524–4530, Oct. 2002.

[7] I. Guedes, N. J. Zaluzec, M. Grimsditch, V. Metlushko, P. Vavassori, B. Ilic, P. Neuzil, and R. Kumar, "Magnetization of negative arrays: Elliptical holes on a square lattice," *Phys. Rev. B*, vol. 62, pp. 11 719–11 724, 2000.

[8] M. Grimsditch and P. Vavassori, "The diffracted magneto-optica Kerr effect: What does it tell you?," *J. Phys.: Condens. Matter.*, vol. 16, pp. R275–R294, 2004.

[9] D. van Labeke, A. Vial, V. A. Novosad, Y. Souche, M. Schelenker, and A. D. D. Santos, "Diffraction light by a corrugated magnetic grating: Experimental results and calculation using a perturbation approximation to the Rayleigh method," *Opt. Commun.*, vol. 124, p. 516, 1996.

[10] M. Grimsditch, P. Vavassori, D. Novosad, V. Metlushko, H. Shima, Y. Otani, and K. Fukamichi, "Vortex chirality in an array of ferromagnetic dots," *Phys. Rev. B*, vol. 65, p. 17 2419, 2002.

[11] I. Guedes, M. Grimsditch, V. Metlushko, P. Vavassori, R. Camley, B. Ilic, P. Neuzil, and R. Kumar, "Domain formation in arrays of square holes in an Fe film," *Phys. Rev. B*, vol. 66, p. 01 4434, 2002.

[12] P. Vavassori, M. Grimsditch, V. Novosad, V. Metlushko, and B. Ilic, "Metaestable states during magnetization reversal in square permalloy rings," *Phys. Rev. B.*, vol. 67, p. 13 4429, 2003.

[13] I. Guedes, M. Grimsditch, V. Metlushko, P. Vavassori, R. Camley, B. Ilic, P. Neuzil, and R. Kumar, "Magnetization reversal in an Fe film with an array of elliptical holes on a square lattice," *Phys. Rev. B.*, vol. 67, p. 02 4428, 2003.

[14] P. Vavassori, V. Metlushko, R. M. Osgood III, M. Grimsditch, U. Welp, and G. Crabtree, "Magnetic information in the light diffracted by a negative dot array of Fe," *Phys. Rev. B.*, vol. 59, pp. 6337–6343, Mar. 1991.

[15] P. Vavassori, V. Metlushko, and M. Grimsditch, "Magneto-optical study of superlattice dot arrays," *Phys. Rev. B.*, vol. 61, pp. 5895–5898, Mar. 2000.

[16] Y. Souche, M. Schelenker, and A. D. Santos, "Non-specualr magneto-optical Kerr effect," *J. Magn. Magn. Mater.*, vol. 140–144, pp. 2179–2180, 1995.

[17] J. L. Costa-Krämer, C. Guerrero, S. Melle, P. García-Mochales, and F. Briones, "Pure magneto-optic diffraction by a periodic domain structure," *Nanotechnology*, vol. 14, pp. 239–244, 2003.

[18] A. Hubert and R. Schäfer, *Magnetic Domains*. Berlin, Germany: Springer-Verlag, 2000.

[19] M. J. Donahue and D. G. Porter. *1999 OOMMF User's Guide Version 1.0*. National Institute of Standards and Technology, Gaithersburg, MD. [Online]. Available: http://math.nist.gov/oommf/

Manuscript received April 13, 2005; revised July 27, 2005.